Int. J. Solids Structures Vol. 14, pp. 625–637

0020-7683/78/0801-0625/$02.00/0

USAGE OF THE TRESCA YIELD CONDITION IN FINITE ELEMENT PLANE STRAIN ANALYSIS

SUBHASH C. ANAND†
Clemson University, Clemson, SC 29631, U.S.A.

and

FRANK E. WEISGERBER‡
University of Pittsburgh, Pittsburgh, PA 15261, U.S.A.

(*Received* 8 *August* 1977; *in revised form* 5 *December* 1977; *received for publication* 1 *February* 1978)

Abstract—Plastic stress–strain relations for perfectly plastic and strain-hardening materials in plane strain condition are developed for materials that obey the Tresca yield condition. A method of handling the three-dimensional yield surface by constructing a two-dimensional equivalent yield surface is described. The plastic stress–strain relations are employed to obtain elastic–plastic solutions for a notched tension specimen subjected to monotonically increasing loads. The results are compared to those previously available in the literature for the von Mises yield condition. It is shown that the stress–strain relations developed for the Tresca yield condition in plane strain can be as easily used as those of the von Mises yield condition, which have commonly been employed. The resulting solution is more conservative and safe, suggesting that it is desirable to use the Tresca yield condition in elastic–plastic analyses of metal structures in design.

INTRODUCTION

The finite element method has often been shown to be well-suited to the solution of problems involving non-linear behavior. This is especially true for problems in plasticity and numerous papers have described solutions to such problems. Reference [1] includes a brief account of the early history of the use of the finite element method in plasticity problems and Refs. [2] and [3] give extensive bibliographies on this topic.

Although the Tresca yield condition has not gone completely unnoticed[1, 3, 4], a survey of the literature indicates that von Mises yield condition has predominantly been used in elastic–plastic finite element analyses. It is apparent that for many materials, and in particular for the commonly used metals, the von Mises yield condition agrees as well with the experimentalty produced yield surfaces as does the Tresca yield condition. However, since the Tresca yield condition is inscribed within the von Mises yield condition, it is more conservative and safe to use the former in actual designs. Furthermore, even though the initial yield surfaces for many materials may generally be established as being smooth, and consequently preferable to work with, recent research[5] indicates that certain loading programs may lead to subsequent yield surfaces which exhibit singularities. Thus, the manner of handling yield functions with singularities becomes even more relevant.

In this paper, elastic–plastic stress–strain relations are developed for the plane strain case and a method particularly suitable to handle the three-dimensional yield surfaces with singularities in plasticity problems is described. These relationships are used to obtain elastic–plastic solutions for a plane strain notched tension specimen subjected to monotonically increasing loads using the finite element technique. The results are compared to those previously available in the literature for the von Mises yield condition.

TRESCA YIELD CONDITION

The Tresca yield condition may be written in terms of the principal stresses as

$$F = [(\sigma_1 - \sigma_2)^2 - \bar{\sigma}^2(\kappa)][(\sigma_1 - \sigma_3)^2 - \bar{\sigma}^2(\kappa)][(\sigma_2 - \sigma_3)^2 - \bar{\sigma}^2(\kappa)] = 0 \qquad (1)$$

†Professor of Civil Engineering.
‡Assistant Professor of Civil Engineering.

in which $\bar{\sigma}(\kappa)$ is twice the maximum permissible shear stress in a material in the plastic state. This yield condition can be represented graphically by a regular hexagonal cylinder with its centroidal axis oriented equidistant from the three principal stress axes σ_1, σ_2, σ_3, as shown in Fig. 1, in which each of the six faces of the hexagonal cylinder is numbered and each edge or corner is identified with a letter.

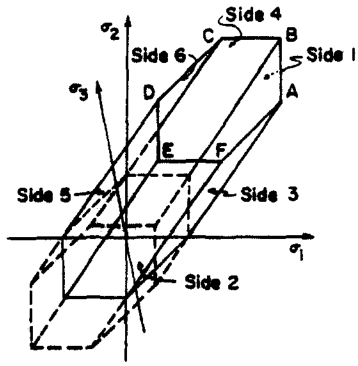

Fig. 1. Three-dimensional Tresca yield surface.

For a perfectly plastic material the yield surface remains unchanged throughout the plastic history of the material. However, the assumption of perfect plasticity generally does not conform to the apparent behavior of real engineering metals as experimental evidence indicates that yield surfaces may change significantly once plastic flow takes place. A long history of experimentation has made it obvious that the relationship between the plastic flow and the kinetics of a yield surface is complex, and cannot be given by a generally acceptable strain-hardening model. Consequently, elastic-plastic solutions employ assumptions of approximate post-yield behavior and the analyst must bear in mind the limitations of the assumptions made.

Isotropic strain-hardening, considered in this paper, is perhaps the simplest post-yield behavior which may be assumed. Under this assumption, the yield surface must always expand with additional plastic flow: it may never contract. The assumption of isotropic strain-hardening does not account for the Bauschinger effect exhibited by most metals when subjected to alternating loads, but it is generally considered satisfactory in association with monotonically increasing loads.

The rate of expansion of a yield surface is governed by the function $\bar{\sigma}(\kappa)$. From the stress-strain curve of a uniaxial test, a plot of $\bar{\sigma}(\kappa)$ vs the plastic component of strain, ϵ^p, may easily be constructed. It is convenient to take the plastic work density as the hardening parameter, i.e.

$$\kappa = \int \sigma_{ij}\, \mathrm{d}\epsilon_{ij}^p \tag{2}$$

which is recognized as the area under the $\bar{\sigma}(\kappa)-\epsilon^p$ curve. Therefore, initial yeild occurs at $\kappa = 0$ and the initial yield stress is denoted by σ_0. The slope of the $\bar{\sigma}(\kappa)-\epsilon^p$ curve, $\mathrm{d}\bar{\sigma}(\kappa)/\mathrm{d}\epsilon^p$, is denoted by H'.

Two materials are considered in this paper: (i) an elastic-perfectly plastic material with $H' = 0$, and (ii) an elastic-strain-hardening material with H' equal to a positive constant.

Specialization for plane strain

It is convenient to expand eqn (1) to a set of six functions, each defining one face of the hexagonal yield surface,

$$\begin{aligned} F^1 &= \sigma_1 - \sigma_3 - \bar{\sigma}(\kappa) = 0 & F^4 &= \sigma_2 - \sigma_3 - \bar{\sigma}(\kappa) = 0 \\ F^2 &= -\sigma_2 + \sigma_3 - \bar{\sigma}(\kappa) = 0 & F^5 &= -\sigma_1 + \sigma_3 - \bar{\sigma}(\kappa) = 0 \\ F^3 &= \sigma_1 - \sigma_2 - \bar{\sigma}(\kappa) = 0 & F^6 &= -\sigma_1 + \sigma_2 - \bar{\sigma}(\kappa) = 0. \end{aligned} \tag{3}$$

For plane strain, defined by

$$\begin{aligned} \epsilon_z &= 0 \\ \gamma_{xz} &= 0 \\ \gamma_{yz} &= 0, \end{aligned} \tag{4}$$

the z-direction is a principal stress direction and the relationships between principal and Cartesian stresses can be written as

$$\begin{aligned} \sigma_1 &= c^2\sigma_x + s^2\sigma_y + 2cs\sigma_{xy} \\ \sigma_2 &= s^2\sigma_x + c^2\sigma_y - 2cs\sigma_{xy} \\ \sigma_3 &= \sigma_z \end{aligned} \tag{5}$$

in which $c = \cos\theta$, $s = \sin\theta$ and θ is the angle from the x-axis to the direction of σ_1 measured positive counter-clockwise. With these relationships, eqn (3) may be specialized in Cartesian coordinates for the plane strain case as

$$\begin{aligned} F^1 &= c^2\sigma_x + s^2\sigma_y + 2cs\sigma_{xy} - \sigma_z - \bar{\sigma}(\kappa) = 0 \\ F^2 &= -s^2\sigma_x - c^2\sigma_y + 2cs\sigma_{xy} + \sigma_z - \bar{\sigma}(\kappa) = 0 \\ F^3 &= (c^2 - s^2)\sigma_x - (c^2 - s^2)\sigma_y + 4cs\sigma_{xy} - \bar{\sigma}(\kappa) = 0 \\ F^4 &= s^2\sigma_x + c^2\sigma_y - 2cs\sigma_{xy} - \sigma_z - \bar{\sigma}(\kappa) = 0 \\ F^5 &= -c^2\sigma_x - s^2\sigma_y + 2cs\sigma_{xy} + \sigma_z - \bar{\sigma}(\kappa) = 0 \\ F^6 &= -(c^2 - s^2)\sigma_x + (c^2 - s^2)\sigma_y - 4cs\sigma_{xy} - \bar{\sigma}(\kappa) = 0. \end{aligned} \tag{6}$$

CONSTITUTIVE RELATIONSHIPS

Elastic stress–strain relations

For plane strain, incremental stresses are related to incremental strains by the standard elastic matrix $\mathbf{D}_0$ as

$$\delta\boldsymbol{\sigma} = \mathbf{D}_0\delta\boldsymbol{\epsilon} \tag{7}$$

in which

$$\begin{aligned} \delta\boldsymbol{\sigma} &= [\delta\sigma_x, \delta\sigma_y, \delta\sigma_z, \delta\sigma_{xy}]^T \\ \delta\boldsymbol{\epsilon} &= [\delta\epsilon_x, \delta\epsilon_y, \delta\epsilon_z, \delta\gamma_{xy}]^T \end{aligned} \tag{8}$$

and $[\ ]^T$ defines the transpose of a matrix. If E and ν define the Young's modulus and the Poisson's ratio of the material, respectively; then, $\mathbf{D}_0$ is given by

$$\mathbf{D}_0 = \frac{E}{(1+\nu)(1-2\nu)}\begin{bmatrix} 1-\nu & \nu & \nu & 0 \\ \nu & 1-\nu & \nu & 0 \\ \nu & \nu & 1-\nu & 0 \\ 0 & 0 & 0 & (1-2\nu)/2 \end{bmatrix} \tag{9}$$

Since $\delta\epsilon_z = 0$, eqn (7) may be reduced to

$$\delta\boldsymbol{\sigma} = \mathbf{D}_r\delta\boldsymbol{\epsilon} \tag{10}$$

in which

$$\begin{aligned} \delta\boldsymbol{\sigma} &= [\delta\sigma_x, \delta\sigma_y, \delta\sigma_{xy}]^T \\ \delta\boldsymbol{\epsilon} &= [\delta\epsilon_x, \delta\epsilon_y, \delta\gamma_{xy}]^T \end{aligned} \tag{11}$$

and $\mathbf{D}_r$ is given by

$$\mathbf{D}_r = \frac{E}{(1+\nu)(1-2\nu)}\begin{bmatrix} (1-\nu) & \nu & 0 \\ \nu & (1-\nu) & 0 \\ 0 & 0 & (1-2\nu)/2 \end{bmatrix} \tag{12}$$

The inverse of eqn (10) is often required and may be written as

$$\delta\epsilon^e = \mathbf{D}_r^{-1}\delta\sigma \tag{13}$$

in which

$$\mathbf{D}_r^{-1} = \frac{1+\nu}{E}\begin{bmatrix} 1-\nu & -\nu & 0 \\ -\nu & 1-\nu & 0 \\ 0 & 0 & 1/2 \end{bmatrix} \tag{14}$$

The superscript, e, is used to emphasize the elastic nature of the strains found from eqn (13).

Plastic stress–strain relations

For a material in the plastic state, relationships between stresses and strains are nonlinear and are stated in the rate form as

$$\dot{\sigma} = \mathbf{D}_p\dot{\epsilon} \tag{15}$$

in which $\dot{\sigma}$ and $\dot{\epsilon}$ are stress-rate and strain-rate vectors respectively, and $\mathbf{D}_p$ is the plastic stress–strain transformation matrix. In numerical solutions, however, not the rate form but an incremental form of (15) is used which may symbolically be described by

$$\delta\sigma = \mathbf{D}_p\delta\epsilon. \tag{16}$$

Determination of an explicit form of $\mathbf{D}_p$ requires the definition of the yield function and a flow rule that may be written as

$$\delta\epsilon^p = \lambda\frac{\partial F}{\partial\sigma} \tag{17}$$

in which $\delta\epsilon^p$ is a vector of incremental plastic strains and λ is a positive scalar constant of proportionality. It is also necessary to assume that small increments of strains are divisible into elastic and plastic components, i.e.

$$\delta\epsilon = \delta\epsilon^e + \delta\epsilon^p. \tag{18}$$

Computation of $\delta\epsilon^e$ from eqn (7) by inversion and substitution into eqn (18) along with eqn (17) yields

$$\delta\epsilon = \mathbf{D}_0^{-1}\delta\sigma + \lambda\frac{\partial F}{\partial\sigma}. \tag{19}$$

This latter expression, along with the differentiation of the yield function, leads directly to the plastic stress–strain matrix associated with that yield function. Note that the Tresca yield condition is expressed as a set of functions given in eqn (6) and it is necessary to develop several plastic stress–strain matrices, $\mathbf{D}_p^i$, one for each function, F^i.

The expansion of eqn (19) for yield function F^i gives

$$\delta\epsilon_x = \frac{1}{E}\delta\sigma_x - \frac{\nu}{E}\delta\sigma_y - \frac{\nu}{E}\delta\sigma_z + \lambda^i\frac{\partial F^i}{\partial\sigma_x} \tag{20a}$$

$$\delta\epsilon_y = -\frac{\nu}{E}\delta\sigma_x + \frac{1}{E}\delta\sigma_y - \frac{\nu}{E}\delta\sigma_z + \lambda^i\frac{\partial F^i}{\partial\sigma_y} \tag{20b}$$

$$\delta\epsilon_z = -\frac{\nu}{E}\delta\sigma_x - \frac{\nu}{E}\delta\sigma_y + \frac{1}{E}\delta\sigma_z + \lambda^i\frac{\partial F^i}{\partial\sigma_z} \tag{20c}$$

$$\delta\gamma_{xy} = \frac{2(1+\nu)}{E}\delta\sigma_{xy} + \lambda^i\frac{\partial F^i}{\partial\sigma_{xy}} \tag{20d}$$

and the total differential of F^i is written in the incremental form as

$$0=\frac{\partial F^i}{\partial \sigma_x}\delta\sigma_x+\frac{\partial F^i}{\partial \sigma_y}\delta\sigma_y+\frac{\partial F^i}{\partial \sigma_z}\delta\sigma_z+\frac{\partial F^i}{\partial \sigma_{xy}}\delta\sigma_{xy}-A^i\lambda^i \tag{21}$$

in which

$$A^i=-\frac{\partial F^i}{\partial \kappa}\,\mathrm{d}\kappa\,\frac{1}{\lambda^i}. \tag{22}$$

Since $\delta\epsilon_z=0$ for plane strain, eqn (20c) may be solved for $\delta\sigma_z$ to give

$$\delta\sigma_z=\nu(\delta\sigma_x+\delta\sigma_y)-E\lambda^i\frac{\partial F^i}{\partial \sigma_z} \tag{23}$$

which is substituted into eqns (20a, b, d) and (21) to yield a reduced set of four independent equations

$$\begin{aligned}
\delta\epsilon_x&=\left(\frac{1-\nu^2}{E}\right)\delta\sigma_x-\nu\left(\frac{1+\nu}{E}\right)\delta\sigma_y+\left(\frac{\partial F^i}{\partial \sigma_x}+\nu\frac{\partial F^i}{\partial \sigma_z}\right)\lambda^i\\
\delta\epsilon_y&=-\nu\left(\frac{1+\nu}{E}\right)\delta\sigma_x+\left(\frac{1-\nu^2}{E}\right)\delta\sigma_y+\left(\frac{\partial F^i}{\partial \sigma_y}+\nu\frac{\partial F^i}{\partial \sigma_z}\right)\lambda^i\\
\delta\gamma_{xy}&=2\left(\frac{1+\nu}{E}\right)\delta\sigma_{xy}+\left(\frac{\partial F^i}{\partial \sigma_{xy}}\right)\lambda^i
\end{aligned} \tag{24}$$

and

$$0=\left(\frac{\partial F^i}{\partial \sigma_x}+\nu\frac{\partial F^i}{\sigma_z}\right)\delta\sigma_x+\left(\frac{\partial F^i}{\partial \sigma_y}+\nu\frac{\partial F^i}{\partial \sigma_z}\right)\delta\sigma_y+\left(\frac{\partial F^i}{\partial \sigma_{xy}}\right)\delta\sigma_{xy}-\left[A^i+E\left(\frac{\partial F^i}{\partial \sigma_z}\right)^2\right]\lambda^i.$$

Equations (24) may be written in the matrix form as

$$\begin{Bmatrix}\boldsymbol{\delta\epsilon}\\ 0\end{Bmatrix}=\begin{bmatrix}\mathbf{D}_r^{-1} & \mathbf{L}^i\\ \mathbf{L}^{iT} & \bar{\mathbf{A}}^i\end{bmatrix}\begin{Bmatrix}\boldsymbol{\delta\sigma}\\ \lambda^i\end{Bmatrix} \tag{25}$$

in which

$$\mathbf{L}^i=\begin{Bmatrix}\left(\frac{\partial F^i}{\partial \sigma_x}+\nu\frac{\partial F^i}{\partial \sigma_z}\right)\\ \left(\frac{\partial F^i}{\partial \sigma_y}+\nu\frac{\partial F^i}{\partial \sigma_z}\right)\\ \left(\frac{\partial F^i}{\partial \sigma_{xy}}\right)\end{Bmatrix} \tag{26}$$

$$\bar{\mathbf{A}}^i=-\left[A^i+E\left(\frac{\partial F^i}{\partial \sigma_z}\right)^2\right], \tag{27}$$

$\boldsymbol{\delta\sigma}$ and $\boldsymbol{\delta\epsilon}$ are given in eqn (11), and $\mathbf{D}_r^{-1}$ is defined in (14). Expansion of eqn (25) gives

$$\boldsymbol{\delta\epsilon}=\mathbf{D}_r^{-1}\boldsymbol{\delta\sigma}+\mathbf{L}^i\lambda^i \tag{28a}$$

and

$$0=\mathbf{L}^{iT}\boldsymbol{\delta\sigma}+\bar{\mathbf{A}}^i\lambda^i \tag{28b}$$

which may be solved simultaneously to yield expressions of λ^i and $\mathbf{D}_p^i$ for plane strain as

$$\lambda^i=\mathbf{M}^{i-1}\mathbf{L}^{iT}\mathbf{D}_r\boldsymbol{\delta\epsilon} \tag{29}$$

and

$$\mathbf{D}_p^i=\mathbf{D}_r-\mathbf{D}_r\mathbf{L}^i\mathbf{M}^{i-1}\mathbf{L}^{iT}\mathbf{D}_r \tag{30}$$

in which

$$\mathbf{M}^i = -\bar{\mathbf{A}}^i + \mathbf{L}^{i^T}\mathbf{D}_r\mathbf{L}^i. \tag{31}$$

It is also necessary to derive the matrices for plastic stress–strain relations that correspond to the corners of the yield surface. The total incremental strains at a corner are given by

$$\boldsymbol{\delta\epsilon} = \mathbf{D}_0^{-1}\boldsymbol{\delta\sigma} + \lambda^i\left(\frac{\partial F^i}{\partial \boldsymbol{\sigma}}\right) + \lambda^j\left(\frac{\partial F^j}{\partial \boldsymbol{\sigma}}\right). \tag{32}$$

Taking the derivatives of both yield functions, F^i and F^j, which intersect to form corner "a", gives

$$0 = \left[\frac{\partial F^i}{\partial \boldsymbol{\sigma}}\right]^T \boldsymbol{\delta\sigma} - A^i(\lambda^i + \lambda^j) \tag{33}$$

$$0 = \left[\frac{\partial F^j}{\partial \boldsymbol{\sigma}}\right]^T \boldsymbol{\delta\sigma} - A^j(\lambda^i + \lambda^j) \tag{34}$$

in which A^i and A^j are defined as

$$A^i = -\frac{\partial F^i}{\partial \kappa}\,\mathrm{d}\kappa\,\frac{1}{(\lambda^i + \lambda^j)}$$

and (35)

$$A^j = -\frac{\partial F^j}{\partial \kappa}\,\mathrm{d}\kappa\,\frac{1}{(\lambda^i + \lambda^j)}.$$

Equations (32)–(34) lead to expressions for λ and $\mathbf{D}_p$ in a manner similar to that used with respect to the sides of the yield surface, i.e.

$$\boldsymbol{\lambda}^a = \mathbf{M}^{a^{-1}}\mathbf{L}^{a^T}\mathbf{D}_r\boldsymbol{\delta\epsilon} \tag{36}$$

and

$$\mathbf{D}_p{}^a = \mathbf{D}_r - \mathbf{D}_r\mathbf{L}^a\mathbf{M}^{a^{-1}}\mathbf{L}^{a^T}\mathbf{D}_r \tag{37}$$

wherein

$$\mathbf{M}^a = -\bar{\mathbf{A}}^a + \mathbf{L}^{a^T}\mathbf{D}_r\mathbf{L}^a \tag{38}$$

and

$$\boldsymbol{\lambda}^a = \begin{Bmatrix}\lambda^i\\ \lambda^j\end{Bmatrix} \tag{39}$$

$$\mathbf{L}^a = [\mathbf{L}^i \,\vdots\, \mathbf{L}^j] \tag{40}$$

$$\bar{\mathbf{A}}^a = -\begin{bmatrix} A^i + E\left(\dfrac{\partial F^i}{\partial \sigma_z}\right)^2 & A^i + E\left(\dfrac{\partial F^i}{\partial \sigma_z}\right)\left(\dfrac{\partial F^j}{\partial \sigma_z}\right) \\ A^j + E\left(\dfrac{\partial F^i}{\partial \sigma_z}\right)\left(\dfrac{\partial F^j}{\partial \sigma_z}\right) & A^j + E\left(\dfrac{\partial F^j}{\partial \sigma_z}\right)^2 \end{bmatrix}. \tag{41}$$

Evaluations of plastic stress–strain matrices

If σ_1 is defined as the major principal stress, then it is necessary to develop explicit expressions of the plastic stress–strain relations for Sides 1–3 and Corners A, B, E and F only. Examination of eqns (30) and (37) reveals that they can be evaluated only if A^i is known for eqn (30), and both A^i and A^j are known for eqn (37). It may be shown [6] that A^i (in either case) and A^j are each equal to H', the slope of the $\bar{\sigma}(\kappa)$ vs ϵ^p curve.

Appropriate substitutions into eqn (30) lead to

$$\mathbf{D}_p{}^i = \frac{E(1-\nu)}{(1+\nu)(1-2\nu)}\left(\begin{bmatrix} 1 & \nu/(1-\nu) & 0 \\ \nu/(1-\nu) & 1 & 0 \\ 0 & 0 & (1-2\nu)/[2(1-\nu)] \end{bmatrix} - \frac{\dfrac{E(1-\nu)}{(1+\nu)(1-2\nu)}}{[H'+2E/(1+\nu)]}\cdot\begin{bmatrix} d_{11} & d_{12} & d_{13} \\ & d_{22} & d_{23} \\ \text{symmetric} & & d_{33} \end{bmatrix}\right), \tag{42}$$

in which *for Side* 1,

$$\begin{aligned} &d_{11} = c^4, \quad &d_{12} = c^2s^2, \quad &d_{13} = c^3s, \\ &d_{22} = s^4, \quad &d_{23} = -c^3s, \quad &d_{33} = c^2s^2, \end{aligned} \tag{43}$$

for Side 2,

$$\begin{aligned} &d_{11} = s^4, \quad &d_{12} = c^2s^2, \quad &d_{13} = -cs^3, \\ &d_{22} = c^4, \quad &d_{23} = -c^3s, \quad &d_{33} = c^2s^2, \end{aligned} \tag{44}$$

for Side 3,

$$\begin{aligned} &d_{11} = (c^2-s^2)^2, \quad &d_{12} = -(c^2-s^2)^2, \quad &d_{13} = 2cs(c^2-s^2), \\ &d_{22} = (c^2-s^2)^2, \quad &d_{23} = -2cs(c^2-s^2), \quad &d_{33} = 4c^2s^2. \end{aligned} \tag{45}$$

Appropriate substitutions into eqn (37), and letting $\eta = H'(1+\nu)/E$, lead to

$$\mathbf{D}_p{}^a = \frac{E(1-\nu)}{(1+\nu)(1-2\nu)}\left(\begin{bmatrix} 1 & \nu/(1-\nu) & 0 \\ \nu/(1-\nu) & 1 & 0 \\ 0 & 0 & (1-2\nu)/[2(1-\nu)] \end{bmatrix} - \frac{1-2\nu}{(1-\nu)(2\eta+3)}\cdot\begin{bmatrix} d_{11} & d_{12} & d_{13} \\ & d_{22} & d_{23} \\ \text{symmetric} & & d_{33} \end{bmatrix}\right), \tag{46}$$

in which *for Corners A and F*,

$$\begin{aligned} d_{11} &= 2c^4+2s^4-2c^2s^2+\eta(s^4) \\ d_{12} &= -c^4-s^4+4c^2s^2+\eta(c^2s^2) \\ d_{13} &= 3c^3s-3cs^3+\eta(-cs^3) \\ d_{22} &= 2c^4+2s^4-2c^2s^2+\eta(c^4) \\ d_{23} &= -3c^3s+3cs^3+\eta(-c^3s) \\ d_{33} &= 6c^2s^2+\eta(c^2s^2); \end{aligned} \tag{47}$$

for Corners B and E,

$$\begin{aligned} d_{11} &= 2c^4+2s^4-2c^2s^2+\eta(c^4+s^4-2c^2s^2) \\ d_{12} &= -c^4-s^4+4c^2s^2+\eta(-c^4-s^4+2c^2s^2) \\ d_{13} &= 3c^3s-3cs^3+\eta(2c^3s-2cs^3) \\ d_{22} &= 2c^4+2s^4-2c^2s^2+\eta(c^4+s^4-2c^2s^2) \\ d_{23} &= -3c^3s+3cs^3+\eta(-2c^3s+2cs^3) \\ d_{33} &= 6c^2s^2+\eta(4c^2s^2). \end{aligned} \tag{48}$$

SOLUTION PROCEDURE

As previously noted, in numerical solutions of elastic–plastic problems, it is convenient to replace the rate form of the constitutive relationship for a material in the plastic state with an incremental form.

The solution may then be obtained by an incremental tangent modulus approach, whereby the load is applied in small increments during each of which the structure is assumed to behave linearly. The stiffness of the structure is modified after each load increment, and the process continued until the desired load level is reached. The solution obtained by this simple technique will always be in equilibrium, but the stresses will violate the yield condition unless special corrective techniques are utilized.

One such corrective scheme is the interpolative scheme which has been described in Ref. [7] for a two-dimensional plane stress yield condition. For the plane strain case, however, a three-dimensional yield condition must be considered. Fortunately, it is possible to construct a two-dimensional yield surface for the plane strain case by considering equivalent stresses and, thus, the referenced corrective scheme becomes directly applicable.

The concept of equivalent stresses is best explained with the aid of Fig. 2, in which hexagon *ABCDEF* represents the intersection of the Tresca yield surface (Fig. 1), with the plane defined by $\sigma_3 = 0$, herein called the "zero-plane". Hexagon $A'B'C'D'E'F'$ indicates the intersection of the yield surface with the "alpha-plane" defined by $\sigma_3 = \alpha$. Point P is the origin of the σ_1, σ_2 and σ_3-axes and lies on both the zero-plane and the centroidal axis of the hexagonal cylinder. Point Q identifies the intersection of this centroidal axis with the alpha-plane and may be taken as the origin of a set of equivalent axes σ_{1BQ} and σ_{2BQ} parallel to the σ_1 and σ_2-axes, respectively. The hexagon $A'B'C'D'E'F'$ may then be considered as a two-dimensional yield surface for any given stress state $(\sigma_1, \sigma_2, \sigma_3)$. The equivalent stresses can be expressed in terms of the principal stresses as

$$\begin{aligned} \sigma_{1BQ} &= \sigma_1 - \sigma_3 \\ \sigma_{2BQ} &= \sigma_2 - \sigma_3. \end{aligned} \tag{49}$$

Functions that describe an equivalent yield surface can be found by substituting eqns (49) into eqns (3) to yield

$$\begin{aligned} F^{1BQ} &= \sigma_{1BQ} - \bar{\sigma}(\kappa) = 0 \\ F^{2BQ} &= -\sigma_{2BQ} - \bar{\sigma}(\kappa) = 0 \\ F^{3BQ} &= \sigma_{1BQ} - \sigma_{2BQ} - \bar{\sigma}(\kappa) = 0 \\ F^{4BQ} &= \sigma_{2BQ} - \bar{\sigma}(\kappa) = 0 \\ F^{5BQ} &= -\sigma_{1BQ} - \bar{\sigma}(\kappa) = 0 \\ F^{6BQ} &= -\sigma_{1BQ} + \sigma_{2BQ} - \bar{\sigma}(\kappa). \end{aligned} \tag{50}$$

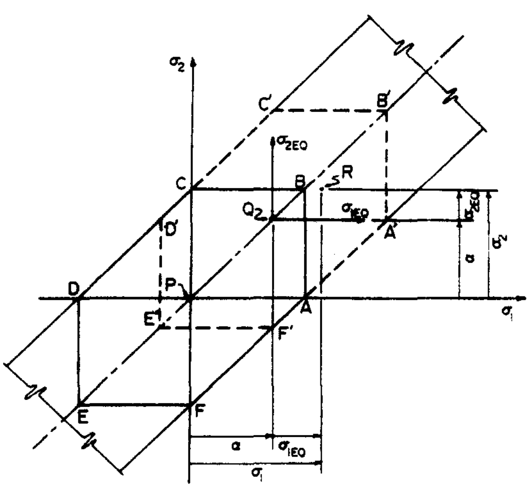

Fig. 2. Equivalent stresses.

Equations (49) and (50) also hold for plane stress conditions, in which $\sigma_3 = 0$. Therefore, the corrective scheme developed for the plane stress case [7] may also be used for the plane strain case. The details of the solution procedure are available in Ref. [7].

NUMERICAL EXAMPLE AND RESULTS

Solutions for a notched tension specimen in plane strain, subjected to a monotonically increasing load, are obtained using the interpolative technique. Both the perfectly plastic material and the strain-hardening material with $H' = 0.032E$ are considered in the analysis. The finite element mesh used in these solutions along with the geometry of the specimen are shown in Fig. 3. Only one quarter of the specimen is used in the model due to the two axes of symmetry that are present.

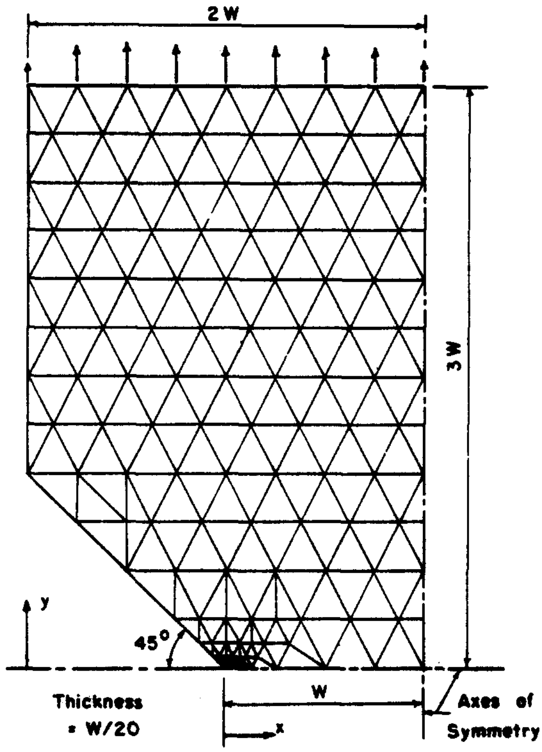

Fig. 3. Finite element mesh for a notched tension specimen.

The progression of plastic enclaves in the specimen at various loads for elastic–perfectly plastic and elastic-strain-hardening materials due to Tresca yield condition are sketched in Fig. 4, which also shows the corresponding enclaves due to von Mises yield condition for elastic-perfectly-plastic materials. The latter have been taken from Ref. [8] and are reproduced here for comparison purposes. The values of load in Fig. 4 are given in a non-dimensional form, i.e. $P/(A \cdot \sigma_0)$, in which P is the total load acting at the end of the specimen, A is the cross-sectional area of the specimen at the notch root and σ_0 is the initial yield stress of the material. An important observation which can be made from a comparison of the enclaves due to usage of the Tresca and Mises yield conditions for elastic-perfectly-plastic materials is that the results obtained by the use of the Tresca yield condition are conservative. For any given magnitude of load, the plastic enclaves for the Tresca yield condition have progressed farther into the specimen than have those due to the von Mises yield condition. Similarly, a plastic enclave which extends completely across the specimen is obtained at a lower load in the case of the Tresca yield condition. This result is in agreement with the fact that the Tresca yield condition is inscribed completely within the von Mises yield condition. The effect of a small amount of strain-hardening in the material on the progression of plastic enclaves due to Tresca yield condition is minimal as the shapes of the enclaves remain almost identical except that their growth rate is retarded somewhat.

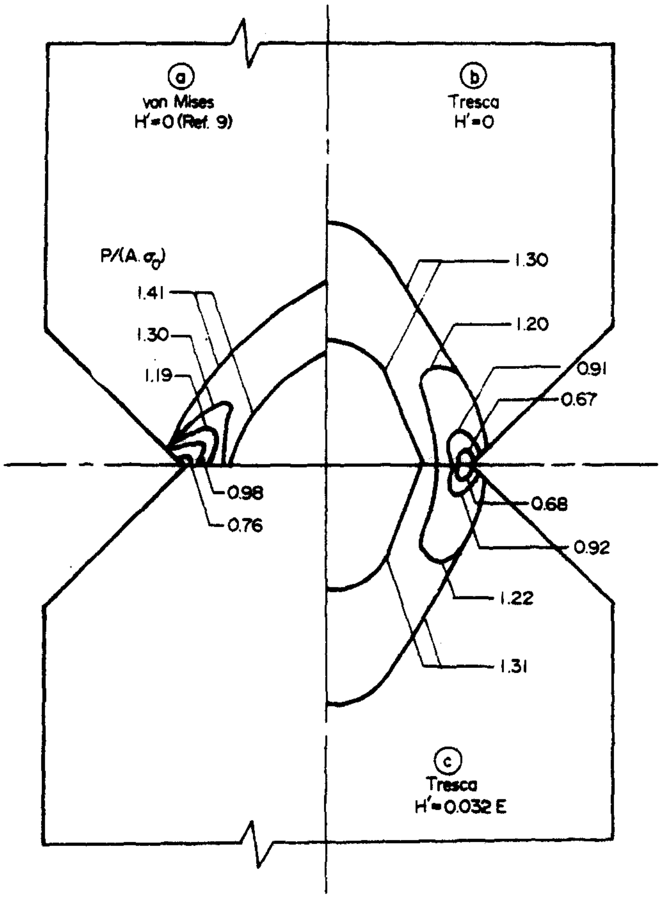

Fig. 4. Progression of plastic enclaves: (a) for perfectly-plastic material obeying von Mises yield condition, from Ref. [9], (b) for perfectly-plastic material obeying Tresca yield condition, (c) for $H' = 0.032E$ and Tresca yield condition.

Strain distributions along the minimum section of the specimen are plotted in Figs. 5 and 6. Though the strains for the strain-hardening case are in general slightly less than those for the perfectly-plastic case, no large effects of the strain-hardening phenomenon are evident. Stress distributions in the specimen for perfectly-plastic and strain-hardening materials are shown in Figs. 7 and 8, respectively. It is obvious that the strain-hardening phenomenon has very little effect on the stress patterns for both σ_x and σ_y. It is of interest to note that σ_y near the notch root exceeds twice the value of $\bar{\sigma}(\kappa)$. This is admissible even for the perfectly-plastic material since normal stresses in the plane strain case may all attain large values without violating the yield condition.

Some effect of strain-hardening is evidenced in Fig. 9 in which longitudinal strains at the notch root are plotted at various loads. The strain-hardening material exhibits less strain for a given load than does the perfectly-plastic material. It should also be noted that the curve for the perfectly-plastic material does not become horizontal even after the plastic enclave has extended completely across the width of the specimen, indicating the capability of the specimen to carry additional load. Incremental loads ranging from 1/10th to 1/80th of the initial yield load were applied in obtaining these solutions for both the perfectly-plastic and strain-hardening cases.

It should be of interest to note that some elements in the plastic regions initially yielded on Side 2 of the Tresca yield condition (Fig. 1) and gradually moved to Side 3 with the increase in load. Stresses in several other yielded elements changed with an increase in load in such a manner that the stress point moved along the edge common to Sides 2 and 3, after initially yielding on Side 2. Such stress points complicate conventional continuum analyses and for that reason the nonlinear von Mises yield condition has been used in such situations. Finite element analyses, on the other hand, are not unduly affected by such stress points, as indicated above,

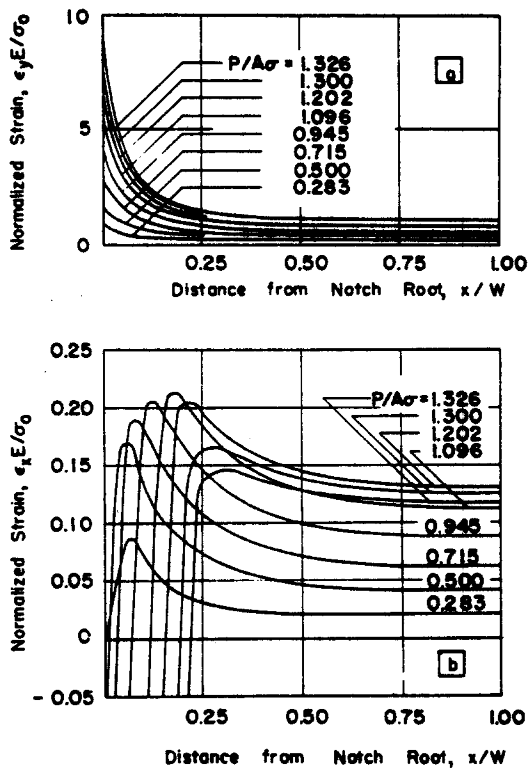

Fig. 5. Strains for perfectly plastic specimen: (a) ϵ_y; (b) ϵ_x.

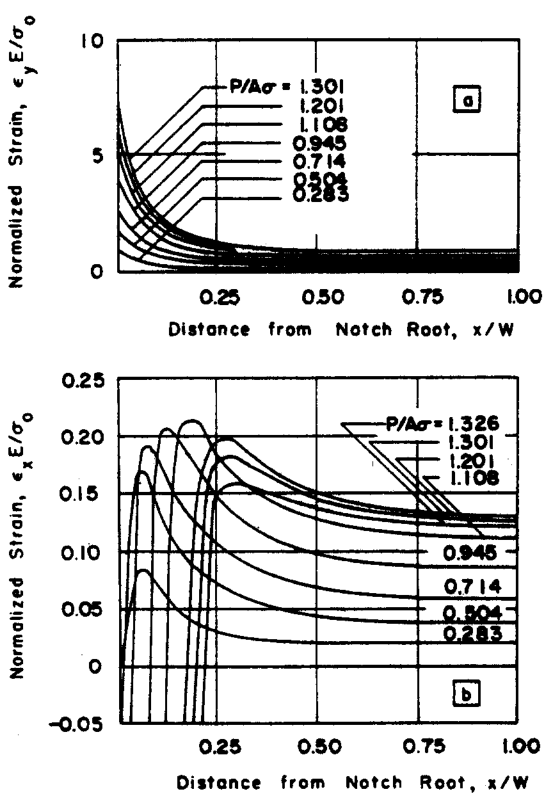

Fig. 6. Strains for strain-hardening specimen: (a) ϵ_y; (b) ϵ_x.

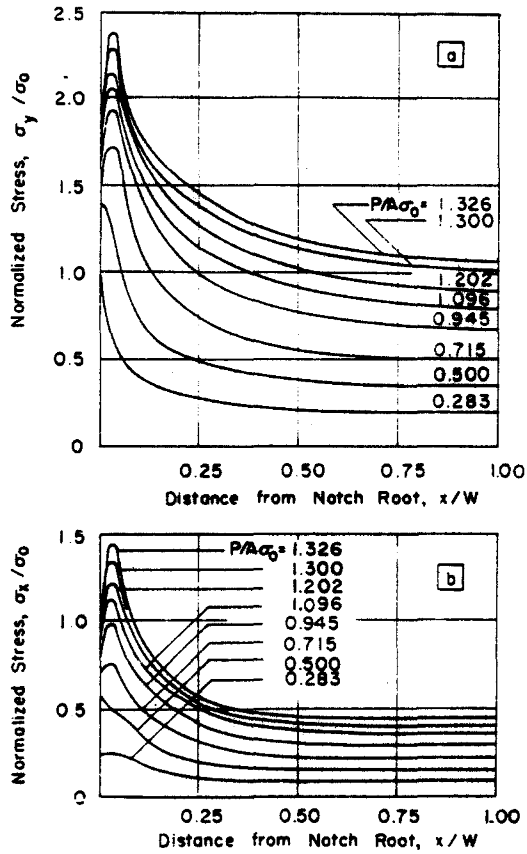

Fig. 7. Stresses for perfectly plastic specimen: (a) σ_y; (b) σ_x.

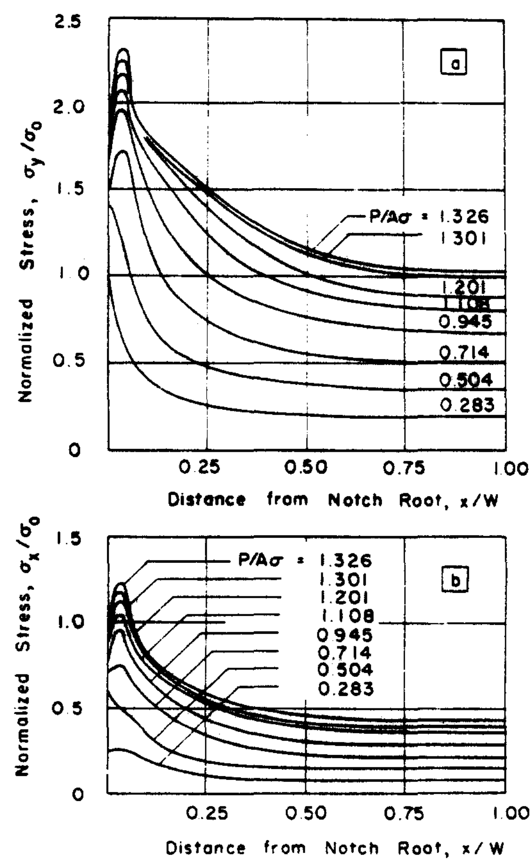

Fig. 8. Stresses for strain-hardening specimen: (a) σ_y; (b) σ_x.

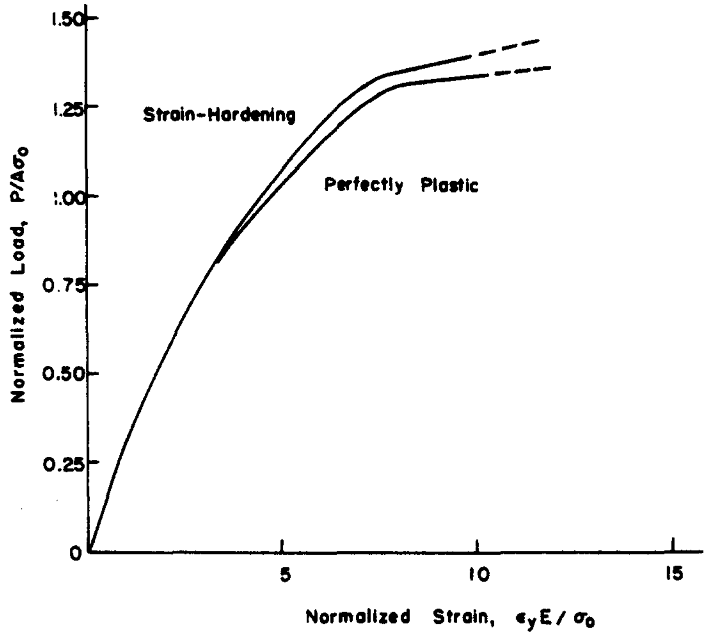

Fig. 9. Load vs strain in y-direction for an element at notch root.

except that schemes to determine which face of the yield surface is involved in plastic flow for a particular element must be built in the computer program.

CONCLUSIONS

It has been shown in this paper that incremental plastic stress–strain relations in plane strain can be easily developed for materials that obey the Tresca yield condition. These relations, expressed in terms of the direction of the major principal stress, can be used to solve elastic–plastic problems by the incremental tangent modulus approach as conveniently as those due to the von Mises yield condition developed by other authors[9]. The points of singularity (corners) in the Tresca yield condition do not present any special problem and the advantages of a smooth yield surface, like Mises', are not obvious. The concept of an equivalent stress permits a redefinition of the yield planes in a convenient form and the solution procedure developed earlier for the plane stress case becomes directly applicable.

The results of the numerical example indicate that the use of the Tresca yield condition leads to loads, for a continuous plastic zone across the notched tension specimen, that are smaller when compared with those obtained by using the von Mises yield condition. Consequently, the Tresca yield condition should be employed in elastic–plastic analyses of metal structures, particularly for those cases where a larger factor of safety need be guaranteed.

REFERENCES

1. S. C. Anand, S. L. Lee and E. C. Rossow, Finite element analysis of elastic–plastic plane stress problems based upon Tresca yield condition. *Ing. Archiv.* **39**, 73–86 (1970).
2. H. Armon, H. S. Levine and A. B. Pifko, Plasticity-theory and finite element applications. *Advances Comp. Meth. Struct. Mech. and Design*, pp. 393–437. Univ. of Alabama Press, Huntsville, Alabama (1972).
3. G. C. Nayak and O. C. Zienkiewicz, Elasto-plastic stress analysis: a generalization for various constitutive relations including strain softening. *Int. J. Num. Meth. Engng* **5**, 113–135 (1972).
4. S. C. Anand and F. E. Weisgerber, Inelastic finite element analysis using Tresca yield condition. *J. Eng. Mech. Div. ASCE* **103**, 1–16 (1977).
5. A. Phillips, Experimental plasticity. Some thoughts on its present status and possible future trends, *Problems of Plasticity*, pp. 193–233. Nordhoff, Leyden (1972).
6. F. E. Weisgerber, Tresca yield condition in elastic–plastic finite element analysis, Ph.D. Dissertation, Clemson University, Clemson (1976).
7. F. E. Weisgerber and S. C. Anand, Interpolative vs iterative solution schemes in elastic–plastic finite element analysis. *Int. J. Num. Meth. Engng.* To be published (1978).
8. O. C. Zienkiewicz, S. Valliappan and I. P. King, Elastic–plastic solutions of engineering problems: "initial stress" finite element approach. *Int. J. Num. Meth. Engng* **1**, 75–100 (1970).
9. Y. Yamada, N. Yoshimura and T. Sakurai, Plastic stress–strain matrix and its applications for the solution of elastic–plastic problems by the finite element method. *Int. J. Mech. Sci.* **10**, 343–354 (1968).